Acquisition of an Insertion Peptide for Efficient Aminoacylation by a Halophile tRNA Synthetase†

Caryn Evilia and Ya-Ming Hou*

Department of Biochemistry and Molecular Biology, Thomas Jefferson University, 233 South 10th Street, Suite 220, Philadelphia, Pennsylvania 19107

Received October 19, 2005; Revised Manuscript Received April 11, 2006

ABSTRACT: Enzymes of halophilic organisms contain unusual peptide motifs that are absent from their mesophilic counterparts. The functions of these halophile-specific peptides are largely unknown. Here we have identified an unusual peptide that is unique to several halophile archaeal cysteinyl-tRNA synthetases (CysRS), which catalyze attachment of cysteine to $tRNA^{Cys}$ to generate the essential cysteinyl-$tRNA^{Cys}$ required for protein synthesis. This peptide is located near the active site in the catalytic domain and is highly enriched with acidic residues. In the CysRS of the extreme halophile *Halobacterium species* NRC-1, deletion of the peptide reduces the catalytic efficiency of aminoacylation by a factor of 100 that largely results from a defect in k_{cat}, rather than the K_m for $tRNA^{Cys}$. In contrast, maintaining the peptide length but substituting acidic residues in the peptide with neutral or basic residues has no major deleterious effect, suggesting that the acidity of the peptide is not important for the k_{cat} of tRNA aminoacylation. Analysis of general protein structure under physiological high salt concentrations, by circular dichroism and by fluorescence titration of tRNA binding, indicates little change due to deletion of the peptide. However, the presence of the peptide confers tolerance to lower salt levels, and fluorescence analysis in 30% sucrose reveals instability of the enzyme without the peptide. We suggest that the stability associated with the peptide can be used to promote proper enzyme conformation transitions in various stages of tRNA aminoacylation that are associated with catalysis. The acquisition of the peptide by the halophilic CysRS suggests an enzyme adaptation to high salinity.

Organisms of hypersaline environments must develop strategies of adaptation to maintain cellular functions in high salt, which severely weakens interactions between many normal mesophilic proteins and their binding partners (*1*, *2*). The issue of adaptation is significantly more challenging for proteins that interact with nucleic acids, due to the polyelectrolyte nature of the latter having the sugar−phosphate backbone (*3*). These proteins constitute every step of the genetic information transfer cascade, from DNA replication to RNA transcription and processing to protein synthesis. An understanding of molecular factors that impart the adaptive ability on halophilic proteins to interact with DNA or RNA is therefore of fundamental importance, particularly for new insights into protein diversity and adaptability that shapes the evolution of life. Here we study aminoacyl-tRNA synthetases (aaRSs),[1] which catalyze aminoacylation of tRNA, to establish the decoding relationships between amino acids and trinucleotide sequences of nucleic acids. Although aminoacyl-tRNA synthetases are essential for life, little is known about how they adapt to high salt, thus leaving a major gap that prevents our understanding of life in high salinity.

Aminoacyl-tRNA synthetases catalyze tRNA aminoacylation in two steps (*4*). The first is activation of an amino acid with ATP to form an enzyme-bound aminoacyl adenylate, with the release of pyrophosphate. The second is transfer of the activated aminoacyl adenylate to the 2′- or 3′-OH of the terminal A76 of the cognate tRNA. There are generally 20 aminoacyl-tRNA synthetases, one for each amino acid, and they are divided into two classes of 10 each, based on different structural folds for ATP binding (*4*). Biochemical studies of these synthetases from halophiles have been difficult, because existing homologous expression systems in halophiles do not produce sufficient quantities of proteins (*5*, *6*). Heterologous expression in *Escherichia coli* typically results in protein precipitation in inclusion bodies, which requires extensive refolding for reactivation of enzymes. While not all synthetases have been successfully refolded, we recently showed that CysRS of the extreme halophile *Halobacterium species* NRC-1 (also known as *Halobacterium halobium* or *Halobacterium salinarium*) can be denatured from inclusion bodies and refolded slowly to exhibit functional activities (*7*). This halophile CysRS, when purified from *E. coli* as a recombinant His-tagged protein, is active at the near-saturating 3.3 M KCl, where it displays kinetic parameters for tRNA aminoacylation in close agreement to those of *E. coli* CysRS (*7*). Recognition of tRNA by this halophile CysRS is also similar to that of *E. coli* CysRS, depending on the conserved U73 and GCA anticodon in $tRNA^{Cys}$ (*7*, *8*), and is facilitated by components of the tRNA tertiary core (*7*, *9*, *10*). Because of the conservation, studies

† This work was supported by NIH Grant GM56662 to Y.-M.H. and Training Grant T32DK07707 that supported C.E.

* To whom correspondence should be addressed. Telephone: (215) 503-4480. Fax: (215) 503-4954. E-mail: Ya-Ming.Hou@jefferson.edu.

[1] Abbreviations: aaRS, aminoacyl-tRNA synthetase; CysRS, cysteinyl-tRNA synthetase; DTT, dithiothreitol; Cys-AMS, 5′-*O*-[*N*-(L-cysteinyl)sulfamoyl]adenosine. All amino acids are shown by the one-letter standard abbreviation code.

10.1021/bi0521386 CCC: $33.50
Published on Web 05/16/2006

of the halophile CysRS can take advantage of available crystal structures of *E. coli* CysRS (*11*, *12*). Thus, the *H. species* NRC-1 CysRS provides an excellent model for addressing halo adaptation of an aminoacyl-tRNA synthetase.

Sequence alignment and structural modeling of the *H. species* NRC-1 (Hh) CysRS (*13*) has identified features that are common to mesophile CysRS and those that are halophile-specific. The common features include class I ATP-binding motifs H[I/L]GH and KMS[K/S]S that are present in all of the halophile CysRS whose sequences are available (Figure 1A, boxed in blue). In crystal structures of *E. coli* CysRS, the ATP motifs lie just outside of the cysteine-binding cleft (Figure 1C), where an enzyme-bound zinc ion recognizes cysteine through a zinc−thiolate interaction (*11*). The zinc ion is coordinated by conserved enzyme side chains that are present in all of the halophile CysRS [C29, C230, H255, and E259 in HhCysRS (Figure 1A, green)]. Once cysteine binds, the zinc ion moves up the cleft while a tryptophan residue swings in to stabilize the bound cysteine. The mobile tryptophan is also conserved (W226, Figure 1A, purple), together with two residues that stabilize the α-amino group of the bound cysteine (G30 and T69, purple). Additionally, the anticodon-binding motif of the *E. coli* enzyme consists of a mixed α/β fold that places six residues within hydrogen bonding distance of the tRNA anticodon (*12*), all of which are present in halophile enzymes [R457, R461, Y466, D470, R473, and D485 (Figure 1A, magenta)]. Finally, recognition of $tRNA^{Cys}$ by *E. coli* CysRS requires an indirect readout mechanism mediated by an asparagine in the C-terminal half that makes contact with backbone residues in the tRNA tertiary core (*12*). This asparagine is also present in the halophile CysRS (N385, Figure 1A, yellow). Interestingly, human CysRS does not use the same indirect readout mechanism to recognize the tRNA core (*14*, *15*), and it contains an aspartic acid instead of asparagine.

The halophile-specific peptide motifs include an insertion peptide of 20 or 21 residues, located between β_3 and α_6 of the catalytic domain (Figure 1A). This insertion peptide is distinct from the eukaryotic-specific insertion peptide of ∼90−100 residues (marked as X_{97} in the human sequence, Figure 1A) and is enriched with acidic residues (20−35%) that are not necessarily conserved in sequence (Figure 1A,B). Other halophile-specific features are clusters of acidic residues in isolated patches, such as D239/D240, D417/E420, and D435/D436 in CysRS of *H. species* NRC-1, which are replaced with neutral residues in *E. coli* CysRS. On the basis of the structure of *E. coli* CysRS, the halophile-specific insertion peptide is predicted to be adjacent to the W226 residue that serves as the gate of the cysteine-binding cleft, whereas the acidic patches are positioned on the surface of the protein opposite from the tRNA-binding site (Figure 1D), suggesting that they have distinct functions. To gain insight into the function of each of these halophile-specific motifs in CysRS of *H. species* NRC-1, we present studies below to test their roles in tRNA aminoacylation and in adaptation to high salinity.

MATERIALS AND METHODS

Recombinant CysRS and Variants of H. species NRC-1. The wild-type construct of the recombinant form of *H. species* NRC-1 CysRS, with an N-terminal His tag, was expressed from the pET-19b vector as described previously (*7*). Mutations of both site-specific substitutions and deletion were created in the gene with the QuikChange kit (Stratagene) and were confirmed by sequence analysis. The wild-type enzyme and all variants were purified from *E. coli* strain BL21/DE3/pSJS according to the previously described denaturation and renaturation procedure (*7*). Concentrations of recombinant enzymes were determined by the active site burst assay (*16*), in a buffer containing 3.5 M KCl, 144 mM Tris-HCl (pH 8.0), 5 μM ATP (1×10^5 cpm of [γ-^{32}P]ATP), 1 mM cysteine, 10 mM $MgCl_2$, 5 mM DTT, and 3 units of pyrophosphatase.

Aminoacylation of tRNA with Cysteine. Assays for tRNA aminoacylation were performed at 40 °C in 3.5 M KCl, 20 mM Tris-HCl (pH 7.5), 1 mM $MgCl_2$, 20 mM DTT, 1 mM ATP, and 20 μM [^{35}S]cysteine (12.5 Ci/mmol) (*7*). The tRNA substrate was made by T7 transcription of the *H. species* NRC-1 $tRNA^{Cys}$ gene and purified on a denaturing gel. The concentration was determined by plateau charging (∼80%). Aminoacylation was initiated with addition of CysRS (0.05 μM wild-type enzyme and 0.5 μM deletion mutant), and aliquots were removed within the linear phase of each time course. The removed aliquots were quenched by carboxymethylation, followed by TCA precipitation on filter pads (*17*). Data of rates versus substrate concentrations were fit to the Michaelis−Menten equation to derive the K_m, k_{cat}, and k_{cat}/K_m parameters. In tRNA-dependent reactions, the tRNA substrate concentration ranged from 0.2 to 8.0 μM while the cysteine concentration was fixed, whereas in cysteine-dependent reactions, the cysteine concentration ranged from 5 to 200 μM while the $tRNA^{Cys}$ concentration was fixed at 15 μM. Due to the limitation of using radioactive cysteine, the amino acid concentration at 20 μM in the assay was not saturating relative to the K_m for cysteine for the wild type and mutants. Thus, the obtained kinetic parameters were deemed apparent parameters.

Salt-Dependent Titration. Aminoacylation of tRNA was assayed in the standard buffer, except with different concentrations of KCl (0.05, 0.5, 0.75, 1.0, 1.25, 1.5, 1.75, 2.0, 2.25, 2.5, 2.75, 3.0, and 3.3 M). Assays were carried out at a near-saturating $tRNA^{Cys}$ concentration (5 μM) with 0.5 or 5 μM wild-type CysRS and deletion mutant so that initial rates were an approximation of k_{cat}. The rate at each KCl concentration was normalized by the maximal rate to build a salt dependence profile.

Fluorescence Measurements. Steady-state fluorescence spectra were collected on a PTI (Photon Technology International, Lawrenceville, NJ) model 814 benchtop continuous spectrofluorometer. Fluorescence emission spectra were obtained by exciting samples at 282 nm and scanning from 300 to 400 nm emission wavelengths at 1.0 nm increments. The excitation and emission monochromators were set at slit widths of 1 mm. The photomultiplier voltage was set at 1100 V, and data were collected using FeliX32 and imported into Excel and Sigmaplot for graphic presentation. Fluorescence emission spectra for the reaction buffer at the appropriate excitation wavelength were obtained and subtracted as background from all spectra. Photobleaching was determined to be minimal on the time scale of these experiments, by using a stir bar during scanning and by ensuring that repetitive measurements yielded the same fluorescence emission intensity. After the emission scan for

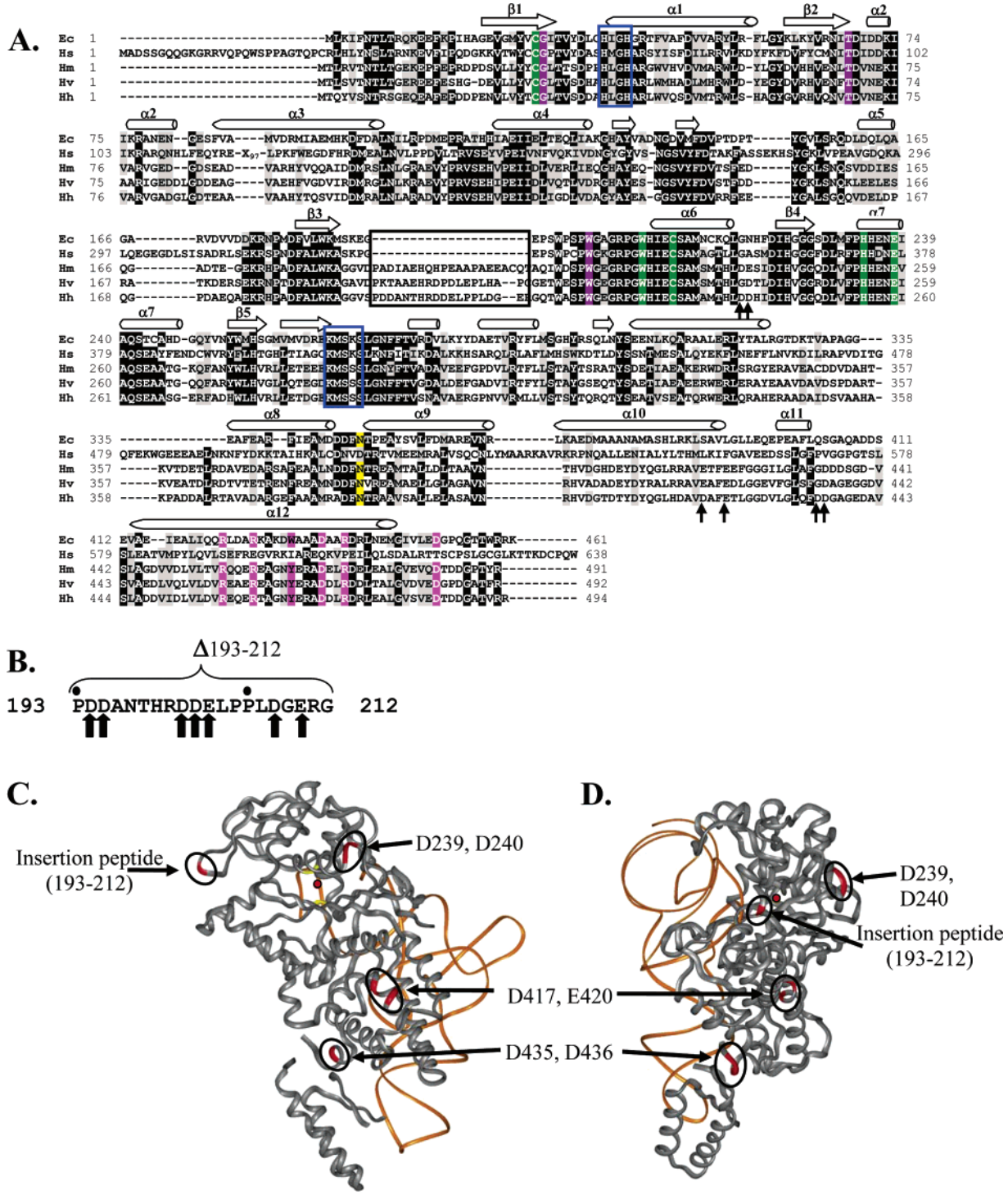

FIGURE 1: (A) Sequence alignment of *E. coli* (Ec), *Homo sapiens* (Hs), *Haloarcula marimosii* (Hm), *Haloferax volcanii* (Hv), and *H. species* NRC-1 (Hh) CysRS. ATP-binding motifs HI/LGH and KMSK/SS are boxed in blue, while ligands to the catalytic zinc ion in the active site are highlighted in green, and those required for stabilization of the α-amino group of cysteine are highlighted in purple. Residues that recognize the $tRNA^{Cys}$ anticodon GCA are highlighted in pink, while the asparagine residue required for indirect readout is highlighted in yellow. The halophile-specific insertion peptide is boxed, while the eukaryotic insertion peptide in the human sequence is indicated by X_{97}. Acidic residues in patches that have been mutated in this study are denoted with arrows. Secondary structural elements of α-helix and *β*-strands based on modeling of crystal structures of *E. coli* CysRS are indicated by horizontal cylinders and arrows on top of the alignment, respectively. (B) The sequence of the halophile-specific insertion peptide of *N. species* NRC-1 CysRS is shown in detail from P193 to G212. The deletion mutant (Δ193−212) refers to elimination of the peptide from P193 to G212, while the ΣAla, ΣAsn, and ΣLys substitution mutants contain replacement of acidic residues in the insertion peptide with the corresponding neutral or basic residues. (C) Crystal structure of the *E. coli* CysRS−$tRNA^{Cys}$ binary complex (*12*), where the enzyme is colored gray and the tRNA orange. Acidic patches D239/D240, D417/E420, and D435/D436 and the predicted position of the insertion peptide are indicated. The active site zinc ion is shown as a red circle. (D) Different view of the *E. coli* CysRS−$tRNA^{Cys}$ binary complex, showing that acid patches are on the surface of the enzyme opposite from the tRNA-binding site.

the enzyme alone [0.1 μM in 3.5 M KCl, 20 mM Tris-HCl (pH 7.5), 5 mM $MgCl_2$, and 1 mM DTT, which yielded 5 × 10^5 counts/s] was obtained, $tRNA^{Cys}$ was added at the indicated concentrations (0.07−7.5 μM), mixed, and allowed

Table 1: Kinetic Parameters for tRNACys by *H. species* NRC-1 CysRS in Aminoacylation

	K_m (μM)	k_{cat} (s^{-1})	k_{cat}/K_m (μM^{-1} s^{-1})	relative k_{cat}/K_m	K_d (μM)
wild type	1.3 ± 0.2	0.11 ± 0.04	0.085	1.0	1.9 ± 0.2
D239A/D240A	1.7 ± 0.4	0.06 ± 0.04	0.034	0.4	
D417A/E420A	1.2 ± 0.01	0.014 ± 0.004	0.012	0.1	
D435A/D436A	2.3 ± 0.9	0.03 ± 0.01	0.014	0.2	
Δ193−212	2.0 ± 1.2	0.0014 ± 0.005	0.0007	0.008	2.2 ± 0.2
ΣAla	2.5 ± 0.6	0.16 ± 0.03	0.064	0.8	1.2 ± 0.1
ΣAsn	5.5 ± 1.2	0.02 ± 0.01	0.004	0.05	
ΣLys	4.4 ± 0.04	0.1 ± 0.01	0.023	0.3	

to bind for 5 min at 25 °C, and the emission scan was observed from 300 to 400 nm. The reactions were carried out at 25 °C during the scan time (approximately 1 min). The changes in intensity at 320 nm versus tRNA concentrations were fit to the hyperbola equation, $y = (a*x)/(x + b)$, where y is the fraction of fluorescence change, x is the concentration of tRNA, a is the plateau of fluorescence change, and b is the K_d for tRNA.

Circular Dichroism Measurements. Circular dichroism spectra were collected on a Cary JASCO J-810 spectropolarimeter. Spectra of CysRS (3.5 μM) in the fluorescence buffer were scanned from 200 to 250 nm, and 50 points were collected at room temperature. Data were normalized using the equation for molar ellipticity: $[\theta] = \theta/(10Cl)$, where θ is in millidegrees, C is in molarity, and l is the path length in centimeters (*18*).

RESULTS

Deletion of the Halophile Insertion Peptide Reduces the k_{cat} of tRNA Aminoacylation. To investigate the functional significance of halophile-specific features, mutations were created that targeted these features in CysRS of *H. species* NRC-1. To test the importance of acidic residues in patches, three double mutants were created to generate mutants D239A/D240A, D417A/D420A, and D435A/E436A. To test the importance of the insertion peptide, a deletion mutant was generated (Δ193−212) in which the P193−G212 peptide was deleted from the wild-type enzyme. To test the importance of acidic residues in the insertion peptide, three substitution mutants in which all seven acidic residues (Figure 1B) between P193 and G212 were replaced with the neutral alanine (ΣAla), asparagine (ΣAsn) or with the basic lysine (ΣLys) were generated. These seven mutants were expressed in *E. coli* and purified from inclusion bodies as the wild-type enzyme to test for their activity of aminoacylation of $tRNA^{Cys}$ with cysteine using the transcript of *H. species* NRC-1 $tRNA^{Cys}$ and [^{35}S]cysteine as the substrates. The aminoacylation assay was performed at the physiologically relevant level of 3.3 M KCl, where the plateau level of charging of the tRNA transcript reached 80%, and the kinetic parameters of the wild-type enzyme (K_m for $tRNA^{Cys}$ of 1.3 μM, k_{cat} of aminoacylation of 0.11 s^{-1}, and catalytic efficiency k_{cat}/K_m of 0.085 μM^{-1} s^{-1}) were in close agreement with those previously published for this enzyme (*7*). Notably, while the K_m for $tRNA^{Cys}$ was similar to that of the mesophilic *E. coli* CysRS (*19*), the k_{cat} was ∼10-fold lower, which was attributed to the suboptimal assay conditions with respect to the nature and concentrations of salts other than KCl. It should be noted that *H. species* NRC-1 is an obligatory extreme halophile that grows in near-saturating salinity (4−5 M salt) (*13*). Although the intracellular concentrations of *H. species* NRC-1 have been estimated to be 1.4 M Na^+, 4.6 M K^+, and 3.6 M Cl^-, there are other organic anions that balanced cations (*20*), whose identities remain unknown at present. These organic anions are difficult to reproduce in vitro.

The concentrations of the seven mutants used in the aminoacylation assay were determined from an active site burst assay. The active fractions of the wild-type enzyme (40%) and of the seven mutants were similar (47% for the ΣLys mutant, 38% for the ΣAsn mutant, 31% for the ΣAla mutant, and 35% for the Δ193−212 mutant), suggesting that the overall folding of these enzymes in the active site was similar. The kinetic parameters of the seven mutants with respect to $tRNA^{Cys}$ in the aminoacylation assay were determined (Table 1). These parameters were obtained by conducting aminoacylation assays at near-saturating concentrations of cysteine (20 μM) and varying concentrations of $tRNA^{Cys}$ to establish relationships between rates and concentrations that could be fit to the Michaelis−Menten equation. Of the seven mutants, the three double mutants were relatively active for aminoacylation, maintaining almost the wild-type K_m and experiencing a small reduction (2−10-fold) in k_{cat}, so that the overall k_{cat}/K_m of these mutants was decreased 2−10-fold. Similarly, the three substitution mutants (ΣAla, ΣAsn, and ΣLys) were also relatively active, as evidenced by their K_m, k_{cat}, and k_{cat}/K_m values being similar to those of the wild type. The most significant defect, however, was observed for the deletion mutant lacking the insertion peptide. This deletion mutant exhibited a nearly 100-fold decrease in k_{cat}, without a major defect on K_m for $tRNA^{Cys}$. The overall loss of catalytic efficiency of aminoacylation was a decrease of 100-fold in k_{cat}/K_m.

Restoration of the insertion peptide, but replacement of acidic residues in the peptide with alanine, asparagine, or lysine, rescued most of the defect of the deletion mutant. For example, in the tRNA-dependent aminoacylation assay (Table 1), the ΣAla and ΣLys substitution mutants nearly restored the k_{cat} completely, bringing the overall k_{cat}/K_m to 80 and 30% of that of the wild type, respectively. The ΣAsn substitution mutant was a little weaker, bringing the overall k_{cat}/K_m to ∼5% of that of the wild type. Of the three substitution mutants, both ΣAsn and ΣLys exhibited an increased K_m for $tRNA^{Cys}$, suggesting an additional factor that influenced the k_{cat}/K_m. The catalytic competence of the ΣAla substitution mutant was confirmed by the cysteine-dependent aminoacylation assay (data not shown). These results suggest that it is the presence of the peptide, but not the acidity or composition of the peptide, that is important for tRNA aminoacylation.

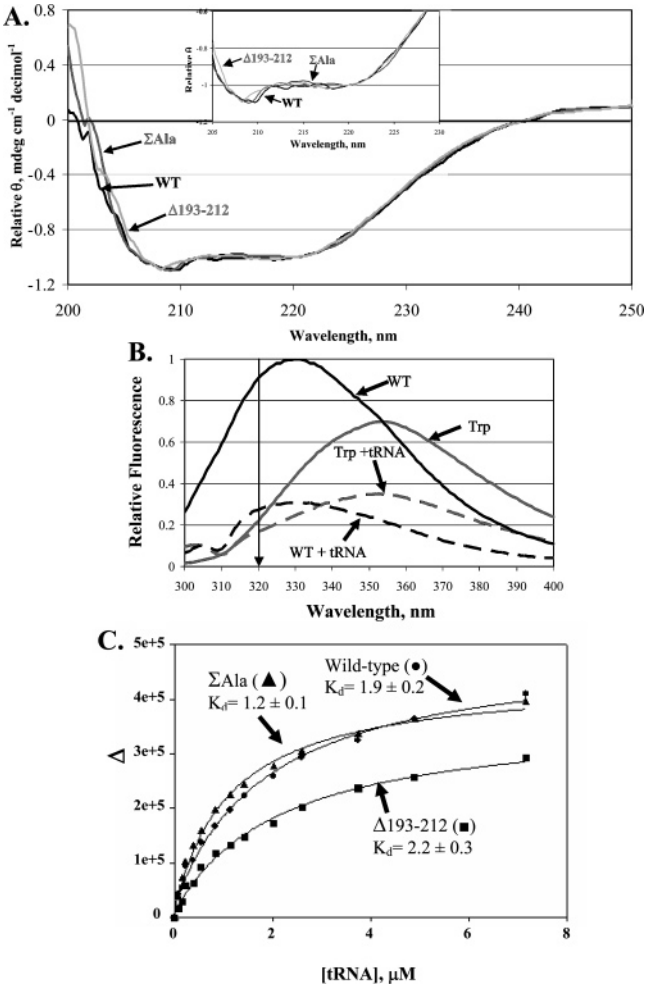

FIGURE 2: (A) Circular dichroism spectra of the wild type, the deletion mutant, and the ΣAla substitution mutant of *H. species* NRC-1. Conditions: 3.5 μM enzyme, 20 mM Tris-HCl (pH 7.5), 3.5 M KCl, 5 mM $MgCl_2$, and 1 mM DTT at 25 °C. (B) Fluorescence emission spectra of wild-type CysRS and a tryptophan solution (both excited at 282 nm) in the absence and presence of $tRNA^{Cys}$. Conditions: 0.1 μM enzyme or 1.3 nM tryptophan, 5 μM $tRNA^{Cys}$, 20 mM Tris-HCl (pH 7.5), 3.5 M KCl, 5 mM $MgCl_2$, and 1 mM DTT at 25 °C. (C) Titration curves of fluorescence emission quenching vs $tRNA^{Cys}$ concentration, fit to a hyperbolic equation, for derivation of the K_d for $tRNA^{Cys}$.

The Deletion Mutant Has a Near-Wild-Type Structure under Physiologically Relevant Salt Conditions. The loss of activity of the deletion mutant was not due to a major change in the global enzyme structure. This was evaluated by two means: using a circular dichroism (CD) spectrum to examine changes in secondary structure content and using the overall tRNA binding affinity as a probe to examine changes in enzyme tertiary structure. The latter was justified on the basis of the cocrystal structure of the *E. coli* CysRS−$tRNA^{Cys}$ complex and was used in a recent study (*12*). Both approaches were examined at the physiologically relevant level of 3.3 M KCl in evaluating structural changes between the wild type and the deletion mutant. The alanine substitution mutant (ΣAla), which had near-wild-type activity, was tested as a control.

The CD spectrum of the wild-type enzyme exhibited the typical ellipticity with a minimum at 220 nm (Figure 2A). This pattern is consistent with the α-helical nature of the protein, as inferred by sequence homology with *E. coli* CysRS, which in the crystal structure is highly rich in α-helices (*11*). The deletion mutant and the catalytically active ΣAla substitution mutant both maintained the shape and amplitude of the wild-type spectrum (Figure 2A), suggesting no global unfolding in either mutant. The affinity of tRNA binding was measured by fluorescence titration, using enzyme tryptophans as an intrinsic probe (Figure 2B). Using the wild-type enzyme as a control, we showed that excitation of the enzyme at 282 nm yielded an emission scan that was quenched by addition of $tRNA^{Cys}$. This quench was specific to CysRS when emission was monitored at 320 nm, because a control solution of tryptophan exhibited a minimal quench by tRNA at this wavelength (Figure 2B). Under the identified excitation and emission conditions, titration of $tRNA^{Cys}$ into the wild-type enzyme progressively quenched the fluorescence intensity, and the decreases in fluorescence intensity at 320 nm versus tRNA concentrations could be fit to a hyperbolic equation to derive a K_d of 1.9 μM for tRNA binding (Figure 2C). This K_d is closely similar to K_m (1.3 μM) in the aminoacylation assay (Table 1). The same titration was performed for the deletion mutant and the ΣAla substitution mutant. The titration curve of the ΣAla substitution mutant was quantitatively similar to that of the wild-type enzyme over the entire range of tRNA concentrations, yielding a similar K_d of 1.2 μM. Interestingly, although the deletion mutant exhibited a much slower increase to reach the plateau of tRNA binding, the K_d was determined on the basis of available data to be 2.2 μM, only slightly higher than that of the wild type. The largely unchanged K_d suggests that the deletion mutant maintained the global structure of the wild-type enzyme and that the catalytic defect of the deletion mutant was not due to a loss in affinity for the tRNA substrate.

The Deletion Mutant Is More Sensitive to Lower Salt Concentrations. Because halophilic enzymes differ from their mesophililc counterparts by having much lower overall hydrophobic content (*21*), the typical salting out/salting in effects of salt to maintain enzyme hydrophobic interiors may not apply (*22*). In addition, the strong affinity of halophilic enzymes for KCl, which is a weak and neutral chaotropic agent, suggests that their salt-dependent activity is not due to salting out/salting in effects but more likely due to salt-induced structural changes. Indeed, studies of several halophilic model systems show that these enzymes coordinate hydrated salt ions on their surface through surface acidic residues and lose activity at lower salt concentrations due to unfolding of structures (*22*−*26*). The salt-dependent activity of aminoacylation was therefore tested and compared among the wild-type enzyme, the deletion mutant, and the ΣAla substitution mutant, to gain insights into differences in their structural stability at lower salt concentrations. The aminoacylation activity was measured as a function of KCl concentration (0−3.3 M), and data were normalized to the maximal activity observed across the range of KCl concentrations (Figure 3A). For all three enzymes, substrate concentrations of near-saturating 20 μM cysteine and saturating 10 μM $tRNA^{Cys}$ were used at all salt concentrations so that the initial rate of aminoacylation was an approximation of k_{cat}. All three enzymes were diluted from a storage buffer of 3.5 M KCl into various salt concentrations and were assayed only when completely solubilized. The wild-type enzyme was soluble at all salt concentrations, whereas the

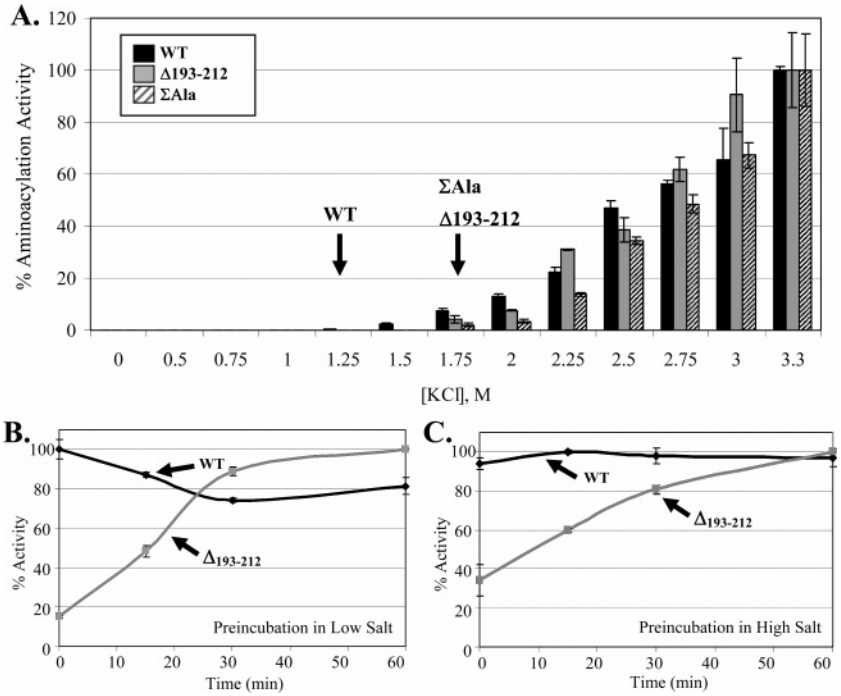

FIGURE 3: (A) Aminoacylation of $tRNA^{Cys}$ (5 μM) by the *H. species* NRC-1 wild-type enzyme (black, 0.5 μM), the deletion mutant (gray, 5 μM), and the ΣAla substitution mutant (striped, 0.5 μM) as a function of KCl concentration. The activity of each enzyme is expressed as a fraction of the maximum, which is at 3.3 M. Each activity is an average of three assays and shown with errors of deviation. The salt threshold for the wild type and mutants is indicated. (B) Aminoacylation of tRNA (5 μM) by the wild-type enzyme (50 nM at 1.75 M KCl) and the deletion mutant (1 μM at 2.0 M KCl) after preincubation at a salt concentration near their respective threshold before the assay for activity. (C) Aminoacylation activity of the wild type and deletion mutant after preincubation at high salt (3.3 M KCl) for the indicated time before the assay for activity.

deletion mutant and the ΣAla substitution mutant rapidly precipitated when diluted to 2.0−0.5 M KCl and were soluble ~30 min after dilution min into the given salt concentration. After the resolubilized mutants were centrifuged at 13000*g* to prove the absence of microscopic precipitation, they were assayed for aminoacylation.

The wild-type CysRS was strongly dependent on salt for aminoacylation; it had no detectable activity at KCl concentrations <1 M but progressively gained activity from <10 to 100% as concentrations of KCl increased from 1.25 to 3.3 M. The threshold of KCl that yielded activity was defined at 1.25 M. This salt requirement was demonstrated previously and was the opposite of the trend of *E. coli* CysRS, the activity of which decreased with increasing KCl concentrations (*7*). Interestingly, although the deletion mutant showed the same overall salt-dependent activities as the wild-type enzyme, exhibiting the maximum activity at 3.3 M KCl, the threshold that allowed detection of activity was higher at 1.75 M KCl (Figure 3A). The same pattern was observed for the ΣAla substitution mutant, with a salt threshold also at 1.75 M KCl (Figure 3A).

The elevated salt threshold for the deletion and ΣAla substitution mutants suggested that they were more sensitive to lowering salts than the wild-type enzyme. To determine if this was related to their propensity to precipitate during dilutions of salt, the wild-type enzyme and the deletion mutant were compared for their stability after incubation at low and high salt over a period of time before the aminoacylation assay (Figure 3B,C). While the wild-type enzyme maintained nearly the same activity after preincubation for 1 h in both low salt (1.75 M KCl) and high salt (3.3 M KCl), the deletion mutant was much more sensitive to salt changes. The activity of the deletion mutant dropped below 20% at the onset of dilution into low salt (from 3.5 to 2.0 M) and dropped below 40% at the onset of dilution into higher salt (from 3.5 to 3.3 M). In both cases, the activity of the deletion mutant progressively improved over time, consistent with the initial occurrence of precipitation that gradually dissolved with time. The analogous behaviors of the deletion and substitution mutants suggested that the sensitivity to salt was a reflection of the absence of acidic residues within the insertion peptide.

The Structural Instability of the Deletion Mutant Is Related to Its Defect in Aminoacylation. The salt sensitivity of the deletion mutant suggested a propensity to unfold. To test this hypothesis, enzyme conformations were probed at different stages of aminoacylation under conditions that would be challenging to structural stability. The rationale was to identify a nonphysiological condition under which the wild-type enzyme would be stable but the deletion mutant would be susceptible to denaturation. The structural probe for this analysis was the intrinsic enzyme tryptophan fluorescence, which arises from a total of eight tryptophans located throughout the entire enzyme sequence and thus provides a tool for monitoring the global enzyme tertiary structure. This would be more informative than the fluorescence change of the single W225, which is limited to active site changes upon cysteine binding. The utility of global fluorescence measurement as a structural probe was demonstrated via examination of the emission spectrum of the wild-type and deletion enzymes in the presence and absence of 7 M urea. The enzyme solution with 7 M urea was prepared by dissolving urea directly into the working buffer containing 3.5 M KCl. The fluorescence analysis showed a

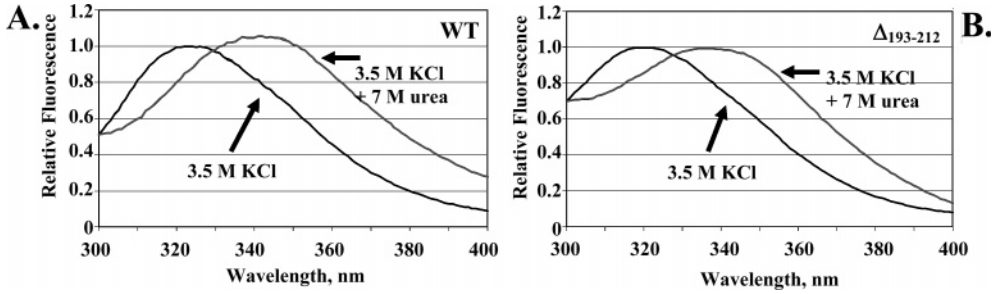

FIGURE 4: Relative fluorescence emission spectra of the *H. species* NRC-1 wild-type enzyme and deletion mutant of CysRS [each at 0.1 μM in 3.5 M KCl, 20 mM Tris-HCl (pH 7.5), 5 mM $MgCl_2$, and 1 mM DTT]. (A) Emission spectra of the wild-type enzyme in the presence or absence of 7 M urea. (B) Emission spectra of the deletion enzyme in the presence or absence of 7 M urea.

shift of the main peak for both enzymes (Figure 4A,B). As a result of the shift, the peak intensity at 320 nm decreased as the concentration of urea increased from 0 to 7 M. The decrease in peak intensity illustrated that the fluorescence emission was sensitive to enzyme conformational changes. To differentiate between the wild-type enzyme and deletion mutant, two conditions were tested. One was to reduce the level of KCl to the threshold concentration for the aminoacylation activity, while the other was to increase concentrations of sucrose. Although both experiments showed the same trend, revealing instability of the deletion mutant, the effects were stronger with sucrose and thus are presented in detail below. In the salt analysis, for example, although complete elimination of salt changed the fluorescence emission of both enzymes, the changes were the same, suggesting that 0 M KCl could not distinguish the two. At 3.5 M KCl (the concentration that yielded the maximum activity for the wild type) and at 1.0 M KCl (the salt threshold for the wild type), while fluorescence emission spectra of the wild type showed no appreciable changes (data not shown), the deletion mutant lost 5% fluorescence peak intensity with the same salt concentration decrease. The inability of the deletion mutant to maintain fluorescence emission like the wild type provided evidence of structural instability, although the 5% loss was smaller compared to the ~20% change when probed in the presence of 30% sucrose.

Sucrose is a common viscogen that increases solvent viscosity without increasing electrolyte charges. This osmolyte also has an effect on the stability and compaction of proteins (*27*). It was directly dissolved into the assay buffer containing the optimum level of 3.5 M KCl so that only the effect of sucrose was examined without changing the salt concentration (Figure 5). Because of the salt, the highest soluble sucrose concentration that was experimentally manageable was 30%. The fluorescence emission spectra of wild-type CysRS were stable in 0−30% sucrose (Figure 5A, left). Although there was a gradual decrease in the peak intensity (at 330 nm) with increasing concentrations of sucrose, the overall decrease was <5% in 30% sucrose (Figure 5C, left), indicating that wild-type CysRS was structurally stable. In contrast, the deletion mutant exhibited an increase in fluorescence intensity as concentrations of sucrose increased (Figure 5B, left). One interpretation of the increase is alteration of the enzyme structure as tryptophan residues became exposed to solution. A nearly 20% increase in the fluorescence peak intensity was observed in 30% sucrose (Figure 5D, left). The inability of the deletion mutant to resist sucrose suggested that it is less stable than the wild type.

Addition of a high concentration (20 μM) of the cysteinyl adenylate analogue, Cys-AMS {5′-*O*-[*N*-(L-cysteinyl)sulfamoyl]adenosine}, to CysRS allowed inspection of the fluorescence change of the enzyme−adenylate complex (Figure 5A,C, middle). In 0% sucrose, the wild-type adenylate complex exhibited a small decrease in fluorescence emission relative to that of the free enzyme, suggesting a small structural rearrangement. This is consistent with crystal structural analysis showing a conformational change of just a mobile tryptophan (W226 in *H. species* NRC CysRS, highlighted in purple in Figure 1A) that rotates into the active site to stabilize the bound cysteine (*11*). As the sucrose concentration increased to 30%, the wild-type adenylate complex exhibited a small increase in fluorescence relative to that in 0% sucrose. The increase in fluorescence suggested a change in conformation, although the amplitude of the change was small, consistent with the ability of the wild-type complex to resist the effect of sucrose. Interestingly, the deletion mutant in the adenylate complex exhibited the same overall change as the wild type (Figure 5B,D, middle). The only difference was observed in 30% sucrose, as the enzyme changed conformation from the free form to the adenylate-bound form. While the wild type exhibited a small increase (5%) upon binding the adenylate analogue, the deletion mutant showed a 20% decrease (Figure 5C,D, middle). The larger-amplitude change provided additional evidence that the deletion mutant was less stable.

Addition of $tRNA^{Cys}$ to the CysRS−adenylate complex allowed inspection of fluorescence changes upon formation of a ternary complex that is analogous to the transition state of aminoacylation. In 0% sucrose, the addition of tRNA to the wild-type adenylate complex led to a substantial quench of fluorescence, reducing the peak intensity by 40% (Figure 5A,C, right). The large quench is consistent with major structural changes induced by tRNA binding, as observed in crystal structures (*12*). As the sucrose concentration increased to 30%, the fluorescence emission of the wild-type ternary complex increased by 10% relative to that in 0% sucrose, indicating the effect of sucrose. Here, the deletion mutant behaved in parallel like the wild type in 0% sucrose, but a smaller effect in 30% sucrose (Figure 5B,D, right). The smaller difference between the deletion mutant and the wild type suggested that the binding of both substrates (Cys-AMS and $tRNA^{Cys}$) in the ternary complex had largely eliminated differences between the two proteins such that the deletion mutant was as resistant to 30% sucrose as the wild type. The substrate-induced stabilization had been noted previously in kinetic studies of *E. coli* CysRS (*19*).

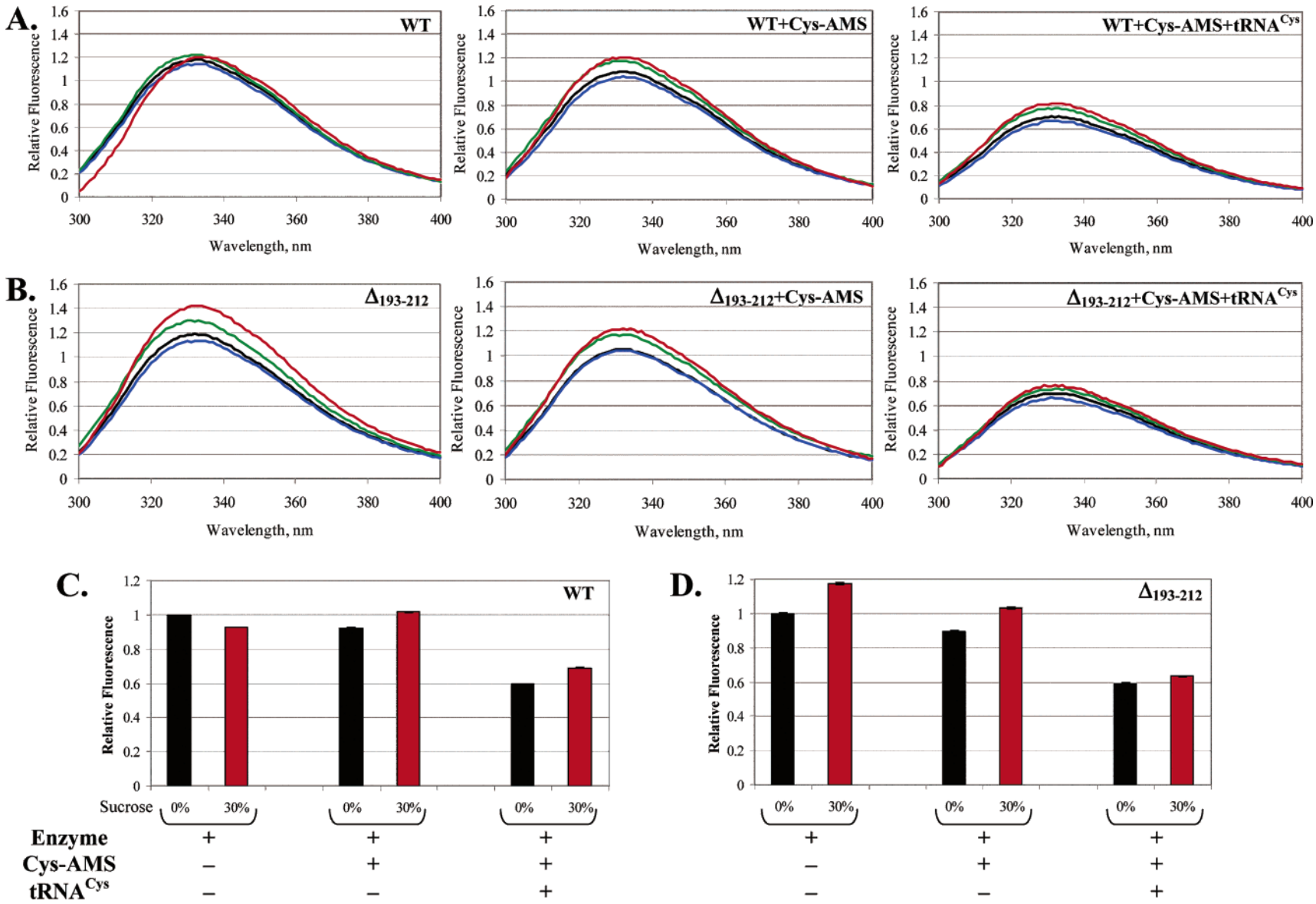

FIGURE 5: Relative fluorescence emission spectra of the *H. species* NRC-1 CysRS (A) wild type and (B) deletion mutant (each at 0.1 μM). The spectra recorded in 0, 10, 20, and 30% sucrose are colored black, blue, green, and red, respectively. Panels on the left are spectra of the enzyme alone, those in the middle spectra of the enzyme−adenylate complex (using the Cys-AMS analogue), and those on the right spectra of the enzyme−adenylate−tRNA^{Cys} ternary complex. (C) Relative fluorescence intensities monitored at 330 nm for the wild type in 0 and 30% sucrose. (D) Relative fluorescence intensities monitored at 330 nm for the deletion mutant in 0 and 30% sucrose. Conditions: 0.1 μM enzyme, 5.0 μM tRNA^{Cys}, and 20 μM Cys-AMS in the buffer described in the legend of Figure 2B. Each fluorescence intensity is an average of three measurements and is reported with errors of deviation (<3%) in panels C and D.

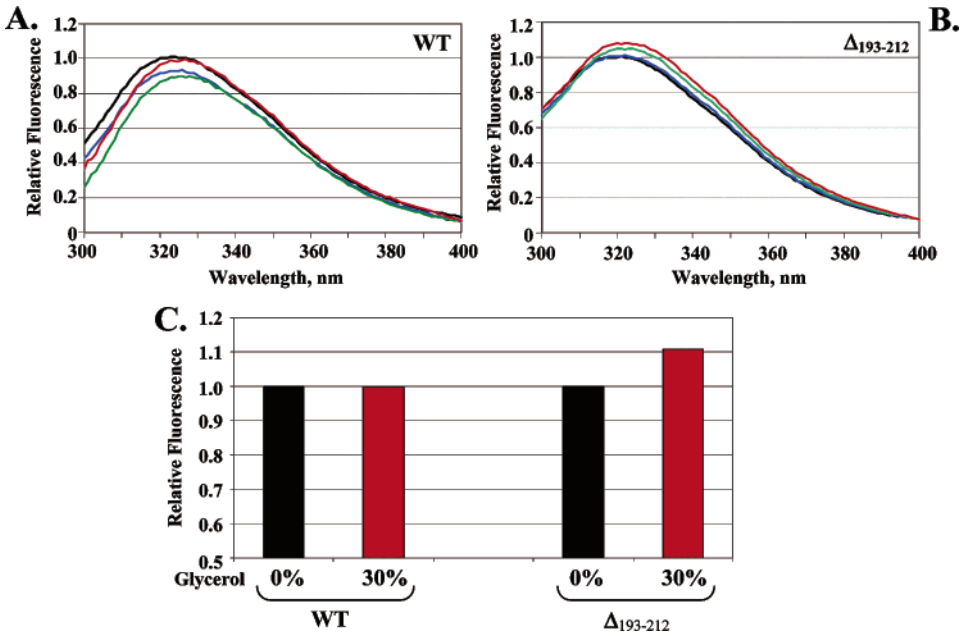

FIGURE 6: Emission spectra of the wild-type enzyme (A) and deletion mutant (B) in 0, 10, 20, and 30% glycerol, which are colored black, blue, green, and red, respectively. (C) Relative fluorescence intensities monitored at 320 nm for the wild-type and deletion enzymes in 0 and 30% glycerol.

To ensure that the effect of sucrose was not due to a chemical effect of the viscogen, a separate viscogen was tested. We chose 30% glycerol, which had a viscosity effect similar to that of 30% sucrose (*28*) and accommodated up to 2.2 M KCl to ensure ~30% of the maximum activity. Fluorescence emission in the presence of 30% glycerol and 2.2 M KCl was examined for both the wild-type and deletion enzymes, but without the Cys-AMS or $tRNA^{Cys}$ substrate, to prevent substrate-induced conformational convergence of the two proteins. Analysis of fluorescence emission confirmed the observation with 30% sucrose: while the wild-type enzyme maintained its spectra as the solution shifted from 0 to 30% glycerol (Figure 6A), the deletion mutant exhibited a 10% increase in peak intensity (Figure 6B). The corroboration of enzyme behaviors in glycerol (Figure 6C) with those in sucrose assured that the observed fluorescence changes did not derive from the chemical effect of a specific viscogen.

DISCUSSION

We have identified an insertion peptide in the *H. species* NRC-1 CysRS that is important for aminoacylation of $tRNA^{Cys}$ with cysteine. This peptide is predicted on the basis of analysis of the *E. coli* CysRS structure to be adjacent to the cysteine-binding site, but not predicted to contact tRNA. Thus, it is interesting that deletion of the peptide has a direct deleterious effect on k_{cat} in the tRNA-dependent aminoacylation reactions (Table 1). There are potentially three explanations for the loss of k_{cat} by deletion of the peptide: (i) global unfolding of CysRS, (ii) loss of substrate affinity, and (iii) loss of enzyme conformational transitions that are associated with catalysis. We have used two independent techniques, CD spectroscopy and fluorescence measurements, to eliminate the first possibility by showing that deletion of the peptide does not cause global unfolding of CysRS under the physiological conditions of 3.3 M KCl (Figure 2). Additionally, we have used fluorescence spectra to monitor binding of tRNA to eliminate the second possibility by showing that deletion of the peptide does not alter the affinity for tRNA in 3.3 M KCl (Figure 2). The focus on the tRNA substrate, rather than cysteine or ATP, is because it is a macromolecule whose binding surface involves a significant portion of the enzyme. Also, the polyelectrolyte nature of tRNA presents it as the most challenging substrate for binding under halophilic conditions (rather than cysteine or ATP). The lack of evidence for unfolding, and the absence of a major effect on tRNA binding, led us to propose that the peptide is involved in conformational transitions of CysRS during catalysis.

The insertion peptide itself is unlikely to be directly involved in catalysis of amino acid activation, because it does not overlap with known catalytic motifs HI/LGH and KMSKS. Neither does the peptide overlap with residues that are involved in stabilization of the α-amino group of cysteine (G30 and T69) (Figure 1A), suggesting that it is unlikely to participate in transfer of the activated aminoacyl group to $tRNA^{Cys}$ based on studies of other synthetases (*29*, *30*). Third, the insertion peptide does not contain residues that are required for coordination of the active site zinc ion (*19*, *31*). Because the active site zinc is predicted to have a catalytic role (*19*), this eliminates a role of the insertion peptide in catalysis mediated by the zinc. These considerations are consistent with our proposal that the insertion peptide is not directly involved in the chemistry step but in facilitating enzyme conformational transitions to facilitate the efficiency of aminoacylation. The magnitude of the effect on k_{cat} by deletion of the peptide (100-fold) is consistent with this proposal. In contrast, residues that are directly involved in catalysis, such as the histidine residues of the HI/LGH motif in MetRS (*32*) or those that coordinate with the catalytic zinc ion in CysRS (*19*), make a contribution to k_{cat} by enhancing it at least 10^3-10^4-fold.

Insights into contributions of the insertion peptide to enzyme conformational transitions come from analysis of

fluorescence emission spectra in 0 and 30% sucrose. The increased solvent viscosity produced by sucrose is a useful probe for monitoring the ability of enzyme conformational transitions and has been exploited for studies of DNA polymerase β (*28*). Although sucrose contains the sugar moiety similar to that in the backbone of tRNA, it is also chemically inert, as demonstrated in studies of the binding interaction between DNA polymerase β and dNTP (*28*). Here, the strongest effect of sucrose is observed with the free enzyme: while the wild type is resistant to changes with 30% sucrose, the deletion mutant is susceptible to a 20% change (Figure 4C,D, left). A second notable difference is observed in the transition from the free enzyme to the enzyme−adenylate complex in 30% sucrose: while the wild type is resistant to change, the deletion mutant undergoes another 20% change (Figure 4C,D, middle). The inability of the mutant to resist sucrose is a clear indication of its structural instability. However, in the ternary complex of CysRS with both the adenylate analogue and $tRNA^{Cys}$, the difference is essentially eliminated (Figure 4C,D, right), suggesting that substrate binding stabilizes the deletion mutant and even repairs its instability. It should be noted that these fluorescence measurements were taken after enzymes and substrates had been mixed in a sucrose solution for an extended time (~1 h). In earlier phases of incubation, while fluorescence spectra of the wild-type enzyme were stable, those of the deletion mutant were unstable (data not shown), suggesting fluctuations of structure. The instability of the deletion mutant can impart a deleterious effect on the steady-state kinetics of aminoacylation, particularly during conformational transitions in various stages of the kinetic pathway.

Enzyme conformational transitions required for catalysis have been identified by analysis of crystal structures of *E. coli* CysRS, and its complexes with cysteine and with $tRNA^{Cys}$ (*11*, *12*). These include (i) rearrangement of the cysteine-binding site upon entry of cysteine and formation of the zinc−thiolate bond, (ii) ordering of the KMSKS loop for synthesis of the cysteinyl adenylate, (iii) ordering of the C-terminal mixed α/β fold for recognition of the tRNA anticodon, and (iv) movement of the enzyme α-helical bundle domain toward the tRNA tertiary core for indirect readout of the tRNA backbone. Interestingly, in the CysRS−tRNA binary complex, the CCA end of the tRNA is misplaced in the ATP-binding site (*12*), suggesting that additional conformational changes are required to remove the CCA end from the ATP-binding site and to properly align catalytic residues for aminoacyl attachment to the CCA end. Presumably, the insertion peptide could be involved in any of these conformational transitions, but it most likely would be involved in steps concerning rearrangement of the active site. This is based on the proximity of the insertion peptide to the cysteine-binding site, which is near the enzyme surface and is one of the most mobile regions during the enzyme catalytic process. The sequence of the insertion peptide provides some clues about how it may facilitate catalysis. For example, it has a relatively fixed length (20 or 21 residues), raising the possibility of a rigid length requirement that brings distant motifs close together. Also, it contains two conserved proline residues, one near the N-terminus of the peptide and the other in the C-terminal half (Figure 1A,B). These two prolines may influence enzyme conformational transitions. The importance of these features will be tested by sited-directed mutagenesis in future work.

The insertion peptide is present in all of the halophile CysRS whose sequence information is available. The peptide is highly enriched with acidic amino acids, but the identities of these acidic residues are not conserved. Analysis of the ΣAla, ΣAsn, and ΣLys mutants also shows that the acidic residues can be changed to neutral or basic residues without any severe effect on the aminoacylation activity at higher salt concentrations. This is in contrast to the conventional thinking that the acidity of halophile proteins is important for enzymatic activities. Thus, it appears that the adaptation of CysRS to halophilic environments is more complicated than a unique peptide or patches of acidic residues. However, we should point out that, while the acidity is not important for tRNA aminoacylation, it is important for halo adaptation. Indeed, the deletion mutant and the ΣAla mutant behave similarly with respect to salt concentrations: both are more sensitive to salt changes, and both are prone to precipitation at nonphysiological salt concentrations (Figure 3). Their higher than wild-type salt threshold for aminoacylation is also consistent with the notion of a less stable structure at lower salt concentrations. It will be interesting to determine if introduction of this insertion peptide to a mesophile CysRS (such as *E. coli* CysRS) might confer adaptability to high salt.

In high-resolution crystal structures of halophilic proteins, clusters of acidic residues are found on protein surfaces, which allow binding with networks of water molecules, and selected ions, so that they stabilize halophilic proteins and permit flexibility under high-salt conditions (*24*, *33*, *34*). The use of an acidic insertion peptide to facilitate halo adaptation has also been proposed for a halophilic ferredoxin (*26*). The halophile CysRS enzymes may have exploited this option further, by acquiring the highly acidic insertion peptide to both improve enzyme stability in high salt and to facilitate conformational transitions associated with catalysis.

ACKNOWLEDGMENT

We thank Dr. Shil DasSarma for providing sequence information of halophile CysRS enzymes and Dr. Howard Gamper and Dr. Chun Mei Zhang for helpful discussion.

REFERENCES

1. Madigan, M. T., and Oren, A. (1999) Thermophilic and halophilic extremophiles, *Curr. Opin. Microbiol. 2*, 265−9.
2. Eisenberg, H., Mevarech, M., and Zaccai, G. (1992) Biochemical, structural, and molecular genetic aspects of halophilism, *Adv. Protein Chem. 43*, 1−62.
3. Lohman, T. M., Overman, L. B., Ferrari, M. E., and Kozlov, A. G. (1996) A highly salt-dependent enthalpy change for *Escherichia coli* SSB protein-nucleic acid binding due to ion-protein interactions, *Biochemistry 35*, 5272−9.
4. Ibba, M., and Soll, D. (2000) Aminoacyl-Trna Synthesis, *Annu. Rev. Biochem. 69*, 617−50.
5. Turner, G. J., Reusch, R., Winter-Vann, A. M., Martinez, L., and Betlach, M. C. (1999) Heterologous gene expression in a membrane-protein-specific system, *Protein Expression Purif. 17*, 312−23.
6. Peck, R. F., Dassarma, S., and Krebs, M. P. (2000) Homologous gene knockout in the archaeon *Halobacterium salinarum* with ura3 as a counterselectable marker, *Mol. Microbiol. 35*, 667−76.
7. Evilia, C., Ming, X., Dassarma, S., and Hou, Y. M. (2003) Aminoacylation of an unusual tRNA(Cys) from an extreme halophile, *RNA 9*, 794−801.

8. Komatsoulis, G. A., and Abelson, J. (1993) Recognition of tRNA-(Cys) by *Escherichia coli* cysteinyl-tRNA synthetase, *Biochemistry 32*, 7435−44.
9. Hamann, C. S., and Hou, Y. M. (1997) An RNA structural determinant for tRNA recognition, *Biochemistry 36*, 7967−72.
10. Hamann, C. S., and Hou, Y. M. (2000) Probing a tRNA core that contributes to aminoacylation, *J. Mol. Biol. 295*, 777−89.
11. Newberry, K. J., Hou, Y. M., and Perona, J. J. (2002) Structural origins of amino acid selection without editing by cysteinyl-tRNA synthetase, *EMBO J. 21*, 2778−87.
12. Hauenstein, S., Zhang, C. M., Hou, Y. M., and Perona, J. J. (2004) Shape-selective RNA recognition by cysteinyl-tRNA synthetase, *Nat. Struct. Mol. Biol. 11*, 1134−41.
13. Ng, W. V., Kennedy, S. P., Mahairas, G. G., Berquist, B., Pan, M., Shukla, H. D., Lasky, S. R., Baliga, N. S., Thorsson, V., Sbrogna, J., Swartzell, S., Weir, D., Hall, J., Dahl, T. A., Welti, R., Goo, Y. A., Leithauser, B., Keller, K., Cruz, R., Danson, M. J., Hough, D. W., Maddocks, D. G., Jablonski, P. E., Krebs, M. P., Angevine, C. M., Dale, H., Isenbarger, T. A., Peck, R. F., Pohlschroder, M., Spudich, J. L., Jung, K. W., Alam, M., Freitas, T., Hou, S., Daniels, C. J., Dennis, P. P., Omer, A. D., Ebhardt, H., Lowe, T. M., Liang, P., Riley, M., Hood, L., and DasSarma, S. (2000) Genome sequence of *Halobacterium species* NRC-1, *Proc. Natl. Acad. Sci. U.S.A. 97*, 12176−81.
14. Lipman, R. S., and Hou, Y. M. (1998) Aminoacylation of tRNA in the evolution of an aminoacyl-tRNA synthetase, *Proc. Natl. Acad. Sci. U.S.A. 95*, 13495−500.
15. Ming, X., Smith, K., Suga, H., and Hou, Y. M. (2002) Recognition of tRNA backbone for aminoacylation with cysteine: Evolution from *Escherichia coli* to human, *J. Mol. Biol. 318*, 1207−20.
16. Fersht, A. R., Ashford, J. S., Bruton, C. J., Jakes, R., Koch, G. L., and Hartley, B. S. (1975) Active site titration and aminoacyl adenylate binding stoichiometry of aminoacyl-tRNA synthetases, *Biochemistry 14*, 1−4.
17. Hou, Y. M., Westhof, E., and Giege, R. (1993) An unusual RNA tertiary interaction has a role for the specific aminoacylation of a transfer RNA, *Proc. Natl. Acad. Sci. U.S.A. 90*, 6776−80.
18. Woody, R. W. (1985) in *The Peptides: Analysis, Synthesis, Biology* (Gross, E., and Meienhofer, J., Eds.) Academic Press, Washington, DC.
19. Zhang, C. M., Perona, J. J., and Hou, Y. M. (2003) Amino acid discrimination by a highly differentiated metal center of an aminoacyl-tRNA synthetase, *Biochemistry 42*, 10931−7.
20. Bayley, S. T., and Morton, R. A. (1978) Recent developments in the molecular biology of extremely halophilic bacteria, *CRC Crit. Rev. Microbiol. 6*, 151−205.
21. Lanyi, J. K. (1974) Salt-dependent properties of proteins from extremely halophilic bacteria, *Bacteriol. Rev. 38*, 272−90.
22. Zaccai, G., Cendrin, F., Haik, Y., Borochov, N., and Eisenberg, H. (1989) Stabilization of halophilic malate dehydrogenase, *J. Mol. Biol. 208*, 491−500.
23. Wright, D. B., Banks, D. D., Lohman, J. R., Hilsenbeck, J. L., and Gloss, L. M. (2002) The effect of salts on the activity and stability of *Escherichia coli* and *Haloferax volcanii* dihydrofolate reductases, *J. Mol. Biol. 323*, 327−44.
24. Madern, D., Ebel, C., and Zaccai, G. (2000) Halophilic adaptation of enzymes, *Extremophiles 4*, 91−8.
25. Ebel, C., Costenaro, L., Pascu, M., Faou, P., Kernel, B., Proust-De Martin, F., and Zaccai, G. (2002) Solvent interactions of halophilic malate dehydrogenase, *Biochemistry 41*, 13234−44.
26. Marg, B. L., Schweimer, K., Sticht, H., and Oesterhelt, D. (2005) A two-α-helix extra domain mediates the halophilic character of a plant-type ferredoxin from halophilic archaea, *Biochemistry 44*, 29−39.
27. Chen, L., Ferreira, J. A., Costa, S. M. B., Cabrita, G. J., Otzen, D., and Melo, E. P. (2006) Compaction of ribosomal protein S6 by sucrose occurs only undernative conditions, *Biochemistry 45*, 2189−99.
28. Bakhtina, M., Lee, S., Wang, Y., Dunlap, C., Lamarche, B., and Tsai, M. D. (2005) Use of viscogens, dNTPαS, and rhodium(III) as probes in stopped-flow experiments to obtain new evidence for the mechanism of catalysis by DNA polymerase *β*, *Biochemistry 44*, 5177−87.
29. Xin, Y., Li, W., Dwyer, D. S., and First, E. A. (2000) Correlating amino acid conservation with function in tyrosyl-tRNA synthetase, *J. Mol. Biol. 303*, 287−98.
30. Xin, Y., Li, W., and First, E. A. (2000) Stabilization of the transition state for the transfer of tyrosine to tRNA(Tyr) by tyrosyl-tRNA synthetase, *J. Mol. Biol. 303*, 299−310.
31. Zhang, C. M., Christian, T., Newberry, K. J., Perona, J. J., and Hou, Y. M. (2003) Zinc-mediated Amino Acid Discrimination in Cysteinyl-tRNA Synthetase, *J. Mol. Biol. 327*, 911−7.
32. Schmitt, E., Panvert, M., Blanquet, S., and Mechulam, Y. (1995) Transition state stabilization by the 'high' motif of class I aminoacyl-tRNA synthetases: The case of *Escherichia coli* methionyl-tRNA synthetase, *Nucleic Acids Res. 23*, 4793−8.
33. Madern, D., Ebel, C., Mevarech, M., Richard, S. B., Pfister, C., and Zaccai, G. (2000) Insights into the molecular relationships between malate and lactate dehydrogenases: Structural and biochemical properties of monomeric and dimeric intermediates of a mutant of tetrameric L-[LDH-like] malate dehydrogenase from the halophilic archaeon *Haloarcula marismortui*, *Biochemistry 39*, 1001−10.
34. Frolow, F., Harel, M., Sussman, J. L., Mevarech, M., and Shoham, M. (1996) Insights into protein adaptation to a saturated salt environment from the crystal structure of a halophilic 2Fe-2S ferredoxin, *Nat. Struct. Biol. 3*, 452−8.

BI0521386